Article:

Bakr, MS orcid.org/0000-0002-2900-8511, Hunter, IC orcid.org/0000-0002-4246-6971 and Bösch, W (2018) Miniature Triple-Mode Dielectric Resonator Filters. IEEE Transactions on Microwave Theory and Techniques, 66 (12). pp. 5625-5631. ISSN 0018-9480

https://doi.org/10.1109/TMTT.2018.2873309

Miniature Triple-Mode Dielectric Resonator Filters

Mustafa S. Bakr, *Student, IEEE*, Ian C. Hunter, *Fellow, IEEE*, and Wolfgang Bsch, *Fellow, IEEE*

***Abstract*—In this paper, a new class of triple-mode microwave filters is presented. These devices use the degenerate pair of the $HE_{11\delta}$ mode and the single $TM_{01\delta}$ mode in dielectric-loaded cavities with unloaded Q-factor of 3000-5000 and reasonable spurious-free window. The proposed structure is obtainable in less than one quarter of the physical volume of equivalent TEM filters. A finite element method solver for electromagnetic structures (HFSS) is used to study the main properties of this resonator. Fundamental design rules for triple-mode bandpass filters with controllable finite transmission zeros are presented. Design examples of bandpass filters with finite transmission zeros on the high or low or both sides of the passband are demonstrated. Measured results demonstrate excellent performance.**

***Index Terms*—Finite transmission zeros, miniaturisation, triple-mode, triplets, and filters.**

I. Introduction

TRIPLY degenerate resonances (triple-mode) occur in structures where symmetry exists in three dimensions, e.g., cubical and spherical structures [1]–[4]. Another approach to the design of triple-mode filters was reported in [5] where higher-order modes were utilised to obtain triply degenerate resonances in waveguide filters; thus, significant size reduction. Similar approach was reported in [6], [7] where higher-order modes were used to obtain triply degenerate resonances in dielectric resonator filters. In [8], the cavity geometry was optimised to design triple-mode filters in dielectric-loaded cavities using the degenerate pair of the TE_{11} mode and the single TM_{01} mode. Traditionally, perturbation methods are required to provide enough coupling between the degenerate modes, i.e., tuning screws or coupling elements, and constitute the filter response. This might degrade the resonator quality factor and increase the design complexity due to the lack of independent control of each resonant frequency and the spurious couplings between the multi-modes. In [9], parallel coupled resonator approach was used to design triple-mode dielectric resonator filters without inter-resonator couplings; thus, simplifying the filter design complexity.

Multi-mode resonators provide the possibility to implement elliptic and pseudoelliptic filter response with minimum number of resonators; therefore, further size reduction [10]. Finite transmission zeros are commonly generated by introducing multiple paths in the structure, i.e., couplings between non-adjacent resonators. This might lead to complex, sensitive and poor temperature stability designs. For instance, when finite transmission zeros are generated close to the passband edge, the direct and cross coupling values can be comparable which might not be realisable in practice. Another example is when the cross-coupling values are so small compared to direct couplings. This can lead to very sensitive designs. Alternatively, nonresonating nodes can be used to generate finite transmission zeros in dual- and triple-mode cavities as reported in [11]. Frequency tuning mechanisms with independent control of each resonance and all inter-cavity couplings are usually required in filter design. This can be a daunting task in multi-mode filters due to the appearance of some spurious couplings between resonances; thus, increasing the design complexity and cost.

In [12], a new class of triple-mode dielectric resonator filters is described that is suitable for base-station applications in less than one quarter of the physical volume of equivalent TEM filters. The proposed resonator consists of a ceramic puck that is placed inside a metallic housing where the bottom surface of the ceramic puck is in contact with the metallic housing. Its geometry was optimised to obtain three non-degenerate modes at the fundamental frequency, i.e., the degenerate pair of the HE_{11} mode and the single TM_{01} mode; thus, significant size reduction. In addition, tuning screws or coupling elements at defined angles were not required to constitute the triple-mode response; thus, greatly simplifying the filter structure, cost and complexity. Finite transmission zeros were generated on the low side of the passband. A prototype hardware was designed, fabricated and measured to validate the proposed approach. However, the operation mechanism of the proposed resonator, control of finite transmission zeros, and higher-order filters were not discussed.

In this paper, The operation mechanism of the triple-mode dielectric resonator filter reported in [12] is explained supported by field components calculations. The generation and control of finite transmission zeros is explained. Fundamental

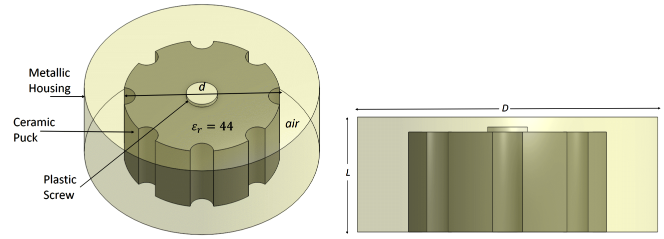

(a) (b)

Fig. 1. Triple-mode dielectric resonator (a) 3D view (b) Cross section view.

Manuscript received Month DD, YYYY; revised Month DD, YYYY; accepted Month DD, YYYY. This paper is an expanded version from the IEEE MTT-S International Microwave Symposium (IMS2018), Philadelphia, PA, USA, June 10-15, 2018. This work was partially supported by the TU Graz LEAD project - Dependable Internet of Things in Adverse Environments, Radio Design Ltd and IEEE Microwave Theory and Techniques Society.

Mustafa S. Bakr is with the Institute of Microwave and Photonic Engineering, Graz University of Technology, Austria; the Institute of Pollard, the University of Leeds, UK; and the Department of Electrical Engineering, University of Technology, Baghdad, Iraq (e-mail: mustafa.bakr@tugraz.at; m.s.a.bakr@leeds.ac.uk).

Ian C. Hunter is with The Pollard Institute, the University of Leeds, UK (e-mail: I.C.Hunter@leeds.ac.uk).

Wolfgang Bsch is with the Institute of Microwave and Photonic Engineering, Graz University of Technology, Austria (e-mail: wbosch@tugraz.at).

design rules of triple-mode bandpass filters are presented followed by design examples showing the control of centre frequency, bandwidth and location of finite transmission zeros. Two filters, a three-pole bandpass filter with two finite transmission zeros on the low side, and a six-pole bandpass filter with four finite transmission zeros on the low side, were designed, fabricated and tested to verify the validity and potential of the proposed resonator. Measured results demonstrate excellent performance.

II. HE-TM Triple Mode Dielectric Resonator Filters

A. Fundamental Design Rules

The approach used in this work is to use a dielectric-loaded cavity which support a single $TE_{01\delta}$ mode at its fundamental frequency, i.e., the dielectric puck is suspended in the middle of the metallic cavity. The geometrical dimensions of the cavity and the position of the dielectric puck are adjusted to support triple-mode resonances, i.e., $HE_{11\delta}$ and $TM_{01\delta}$ modes, at the fundamental frequency as shown in Fig. 6. This enables fourfold size reduction compared with equivalent TEM filters, i.e., air-filled coaxial filters with comparable Q-factor, and good spurious performance. First, a puck suspended in the middle of a metallic housing was moved down towards the base of the housing. Thus, $TE_{01\delta}$ moves up in frequency and $HE_{11\delta}$ moves down in frequency. When the puck is in contact with the base of the housing, $HE_{11\delta}$ is the fundamental frequency. The poor spurious window can be improved by the optimal choice of puck/cavity dimensions as well as reshaping the puck. Finally, the top flat surface of the metallic housing was moved down. The effect of reducing the cavity height is to drive the TM_{01} mode down in frequency while not significantly affecting the other modes and spurious window (Fig. 2). However, it does reduce the Q-factor of the resonator, in particular of the TM_{01} mode (Fig. 3). It is also noted that the E field of the three resonances is maximum near the top flat surface of the resonator where the E field intensity of the TM_{01} mode is significantly larger than the HE_{11} mode (Fig. 6). This drives the TM_{01} mode down in frequency and facilities strong couplings between the three resonances,

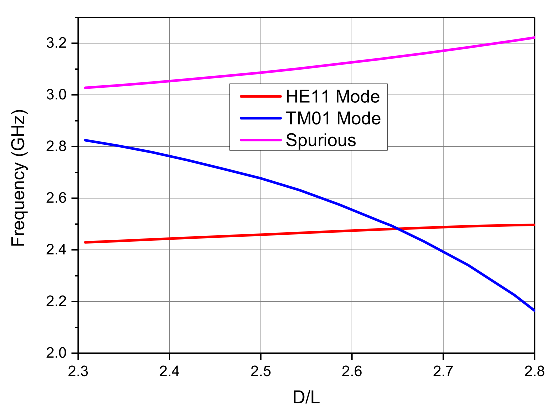

Fig. 2. Mode chart of the triple-mode structure as a function of the ratio of cavity diameter (D) to the cavity height (L) where D = 30 mm.

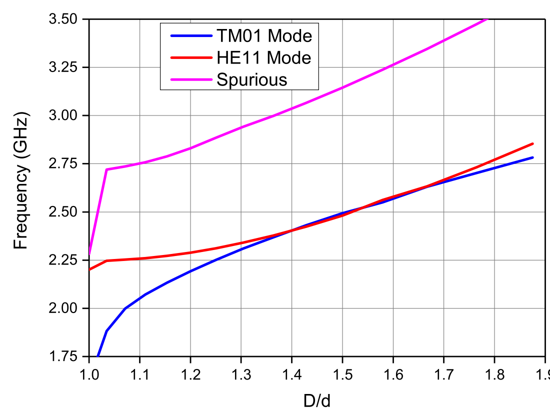

Fig. 4. Mode chart of the triple-mode structure as a function of the ratio of the cavity diameter (D) to the puck diameter (d) where D = 30 mm.

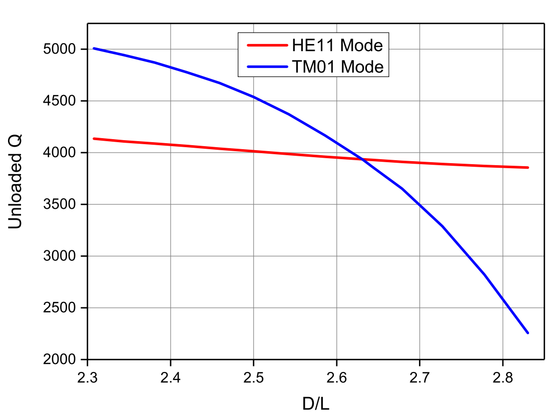

Fig. 3. Unloaded Q chart of the triple-mode structure as a function of the ratio of the cavity diameter (D) to the cavity height (L) where D = 30 mm.

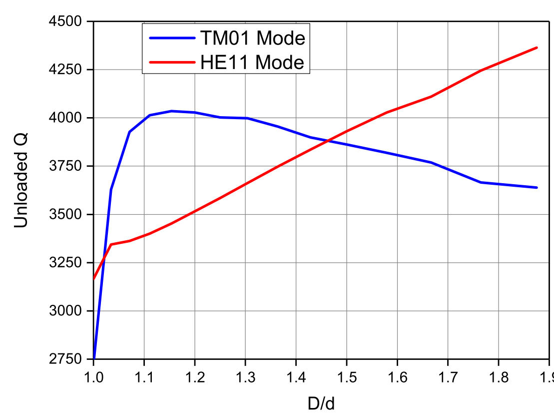

Fig. 5. Unloaded Q chart of the triple-mode structure as a function of the ratio of the cavity diameter (D) to the puck diameter (d) where D = 30 mm.

which is required for base-station filters. Likewise, the effect of adjusting the resonator diameter, where the cavity diameter is defined as D = 30 mm, is presented in Fig. 4. Increasing the resonator diameter drives the first three resonances down in frequency. The unloaded Q-factor of the HE_{11} mode is significantly improved. It is noticed that the Q-factor of the TM_{01} mode is reasonably constant for small cavity to puck diameter ratio (D/d) as depicted in Fig. 5. The mode and unloaded Q-factor charts are used to design bandpass filters using the proposed resonator as the basic building block.

B. Field Components

A finite element method field simulator (HFSS) was used to study the E and H field patterns of the first three resonances of the proposed triple-mode dielectric resonator. Fig. 6 shows the E field intensity of the first three resonances (HE_{11} and TM_{01}) with/without the presence of the input/output probes. It is apparent that the three resonances are orthogonal and uncoupled to each other without any perturbation, such as input/output probes, corner cuts, tuning screws and etc. It is also significant that the axial E field of the three resonances is maximum near the top of the ceramic puck. This facilitates the relatively strong inter-resonator couplings that are required for base-station filters. The field pattern of the first three resonances is relatively constant along the axis of the dielectric. Thus, the resonator resonant frequency is largely determined by the dielectric constant and the diameter of the puck, while it is relatively less dependent on the height of the puck. The unloaded Q-factor of the resonator is mainly determined by the height of the puck and the separation of the puck from the metallic housing. It is also interesting to notice that the presence of the input/output probes is similar to introducing perturbations and breaking the degeneracy of the resonator. This is due to the fact that the E field of the first three resonances is strong in the small gap between the the puck and the cavity, in particular the TM_{01}, and the fact that the three resonances exhibit different polarisations. This enables the design of triple-mode filters without the need to introduce any extra circuits to break degeneracy and provide inter-resonator couplings. Thus, reducing the design complexity and cost. Table I shows the resonant frequency of the first four resonances with/without the presence of the input/output probes. It is apparent that the first three resonances are perturbed in the presence of the input/output probes. This is similar to introducing a discontinuity at 45° in degenerate dual-mode resonators, e.g. TE_{11}, and provide the required inter-resonator coupling.

TABLE I
THE FIRST FOUR RESONANT MODES WITH/WITHOUT THE PRESENCE OF INPUT/OUTPUT PROBES

Mode	f_r (GHz) without input/output probes	f_r (GHz) with input/output probes
HE_{11}	2.38	2.37
HE_{11}	2.38	2.4
TM_{01}	2.38	2.43
Spurious	3.05	3.05

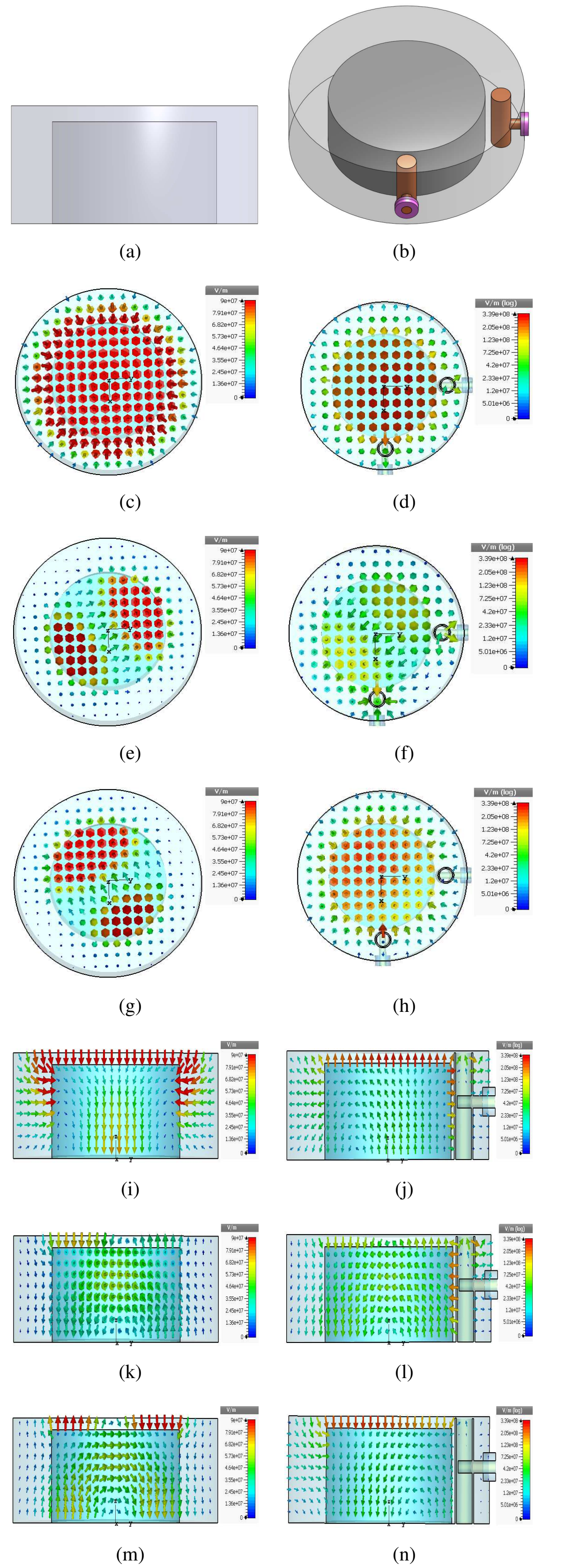

Fig. 6. E field patterns of the triple-mode dielectric resonator (a) Without perturbation, (b) Perturbation (input/output probes); Top and side view of the first three resonances (c, e, g, i, k, and m) TM_{01} and HE_{11} of case a, and (d, f, h, j, l, and n) TM_{01} and HE_{11} of case b.

C. Coupling Scheme

As explained earlier, the required inter-resonator couplings can be simply realised by introducing a proper input/output coupling configuration without the need for any extra coupling elements. The strength of input to resonator couplings, named R_{i1}, R_{o2}, M_{i3}, and M_{o3} in Fig. 7, is mainly controlled by adjusting the height of the input/output probes and the separation of the probes and puck. The sign of couplings is determined by choosing the proper type of input/output configuration, i.e. capacitive or inductive. The inter-resonator couplings between the TM_{01} and the HE_{11}, named M_{23}, exist in the presence of the input/output probes, Fig. 7(a). The internal coupling between the degenerate pair of the HE_{11} resonances, named M_{12}, is negligible due to the symmetry of the structure and the fact that no discontinuity is introduced to perturb the degeneracy of the HE_{11} resonance. Fig. 7 shows the coupling diagram and coupling matrix of the proposed triple-mode dielectric resonator filter. The resonator can be modelled as two cascaded triplets. This enables the realisation of finite transmissions zeros as will be shown in the next section. The input to resonator coupling coefficients can be determined from the filter group delay response as shown in Fig. 8. It is apparent from the balanced group delay response that the input probe excites two resonances at the same time. This result agrees with the coupling scheme shown in Fig. 7.

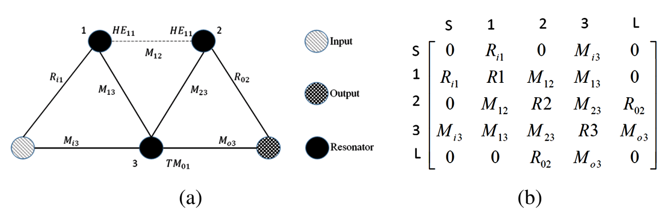

Fig. 7. (a) Cascaded triplets (b) Coupling matrix.

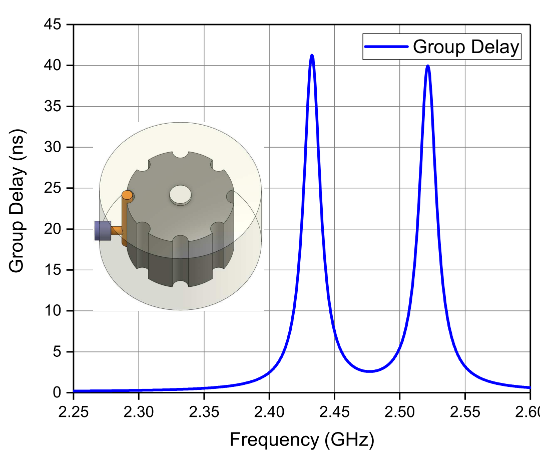

Fig. 8. Group delay response of the probe coupling.

III. Design Examples and Experimental Results

Based on the analysis presented earlier, four bandpass filters are designed to show the potential of the proposed resonator. The first design example shows a three-pole bandpass filter with two transmission zeros on the low side. The second example is a three-pole bandpass filter with one finite transmission zero on both sides. The third design example is a triple-mode bandpass filter with two finite transmission zeros on the high side. Finally, the fourth design example is a six-pole bandpass filter with four finite transmission zeros on the low side.

A. Filters with Two Finite Transmission Zeros on the Low Side

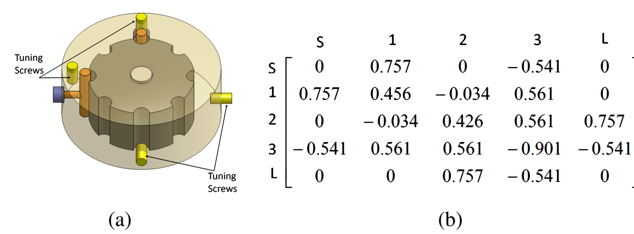

Fig. 9. (a) Triple-mode DR filter with inductive coupling configuration (b) Its coupling matrix.

As a design example, a three-pole bandpass filter was designed and fabricated with a 20 mm diameter and 10 mm height of ceramic puck with permittivity of 44 and loss tangent of 4×10^{-5} in a cylindrical copper cavity with internal dimensions of 30 mm diameter and 11.35 mm height with electrical conductivity of 4×10^{7} S/m. The fundamental frequency was 2.5 GHz with unloaded Q-factor of 3800. The first spurious mode happened 650 MHz above the fundamental frequency. Fig. 9 shows a photo of the 3D model of the triple-mode dielectric resonator filter with inductive coupling configuration and its calculated coupling matrix. The resonator is synthesised as two cascaded triplets. The individual cou-

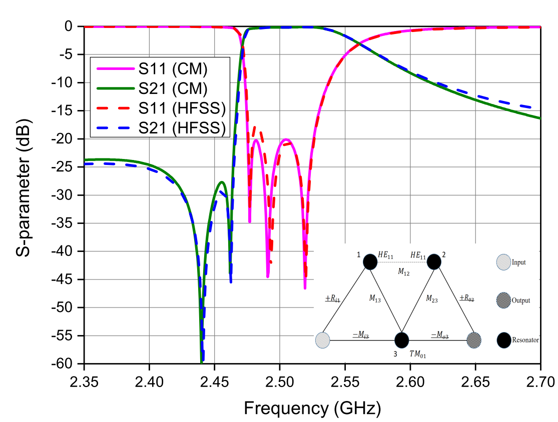

Fig. 10. EM simulation versus coupling matrix frequency response with two finite transmission zeros on the lower side.

plings needed to design a three-pole bandpass filter may be better understood by looking at the E field of each of the first three resonances and the group delay response shown in

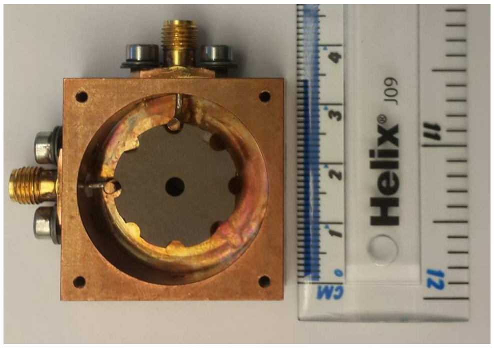

Fig. 11. Photo of triple-mode bandpass filter with two finite transmission zeros on the low side.

Fig. 6 & 8 respectively. The axial E field of the TM_{01} is relatively constant and maximum near the top of the ceramic puck. The input to resonator (TM_{01}) coupling strength and sign (M_{i3} and M_{o3}) are mainly determined by adjusting the height and type of the input/output probes. Similarly, the input to resonator (HE_{11}) coupling strength and sign (R_{i1} and R_{o2}) are mainly determined by adjusting the separation of the input/output probes and puck as well as the coupling type, i.e. capacitive or inductive. The filter bandwidth and location of finite transmission zeros are determined by controlling the strength and sign of the aforementioned couplings. The

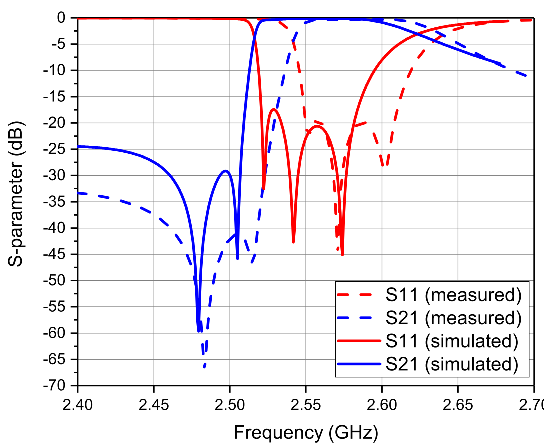

Fig. 12. EM simulation versus measured frequency response with two finite transmission zeros on the lower side.

longitudinal grooves in the ceramic puck are introduced to achieve the required R_{i1} and R_{o2} couplings and meet the given specifications. A comparison between the simulation and synthesised frequency response is shown in Fig. 10. A prototype bandpass filter has been designed, fabricated and measured to validate the proposed approach. The basic specification was chosen as 50 MHz ripple bandwidth at 2.5 GHz centre frequency with insertion loss less than 0.17 dB and out of band rejection of 25 dB at 2.46 GHz. A three pole generalised Chebyshev filter with two finite transmission zeros on the low side is required to meet the chosen specifications. A photograph of the fabricated prototype is shown in Fig. 11. The filter response was tuned using four metallic tuning screws. The resonant frequencies of the HE_{11} modes were tuned using two metallic screws from the side walls. Couplings from the input to the first three resonances were adjusted using the metallic screws that are placed on the top lid of the metallic housing. A comparison between the simulation and measured frequency response is shown in Fig. 12. In comparison to the simulation result, the measured frequency response is slightly shifted up in frequency by approximately 20 MHz. This shift in frequency is believed to originate from inaccuracies due to the tolerance in the dielectric constant of the used off-the-shelf ceramic puck. The filter frequency response was

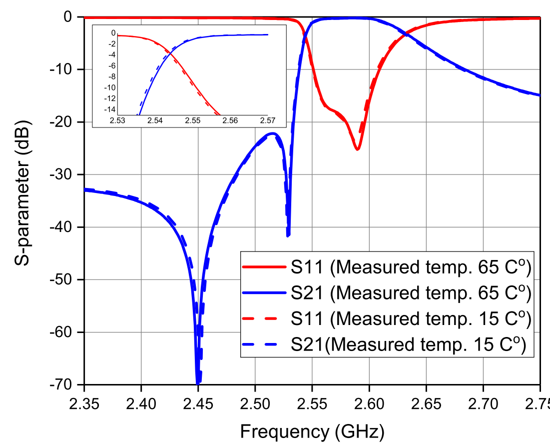

Fig. 13. Measured frequency response of the triple mode filter with temperature.

measured as a function of temperature in the range of 15 to 65 C^o. Fig. 13 shows the measured frequency response at two temperature ranges, i.e. 15 and 65 C^o. The total frequency deviation with temperature was only 0.4 MHz. In addition, the three fundamental resonances seem to drift in the same direction with temperature.

B. Filters with Balanced Shoulders

The basic specification for this filter was chosen as 20 MHz ripple bandwidth at 2.48 GHz centre frequency with insertion loss less than 0.4 dB and out-of-band rejection of 25 dB at 2.45 GHz and 2.51 GHz. This requires the design of balanced shoulder (elliptical response) filters. To locate the finite transmission zeros on both sides, the sign of couplings in one of the cascaded triplets can be altered. It is well-known that each triplet is responsible for the location of one finite transmission zero either on the low or high side. In this design example, the sign of M_{o3} coupling is changed from - to +. To achieve this, the resonant frequency of the TM_{01} mode is defined in the middle of the three fundamental resonances. In addition, unlike the input probe, the output probe is not grounded. Fig. 14 shows a photo of the 3D model of the triple mode filter with inductive and capacitive coupling configuration and its coupling matrix. A comparison between the simulation and synthesised filter response is shown in Fig. 15.

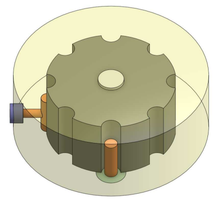

(a)

	S	1	2	3	L
S	0	0.994	0	0.41	0
1	0.994	−0.697	0	0.886	0
2	0	0	0.761	0.886	0.994
3	0.41	0.886	0.886	−0.038	−0.43
L	0	0	0.994	−0.43	0

(b)

Fig. 14. (a) Triple-mode DR filter with inductive and capacitive coupling configuration (b) Its coupling matrix.

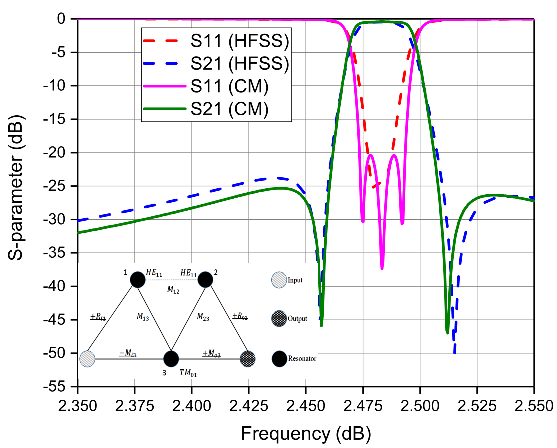

Fig. 15. EM simulation versus coupling matrix frequency response with one finite transmission zero on each side.

C. Filters with Two Finite Transmission Zeros on the High Side

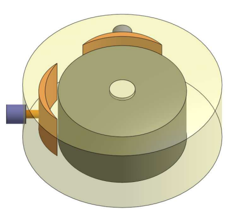

(a)

	S	1	2	3	L
S	0	−0.768	0	−0.666	0
1	−0.768	−0.479	0.0252	0.478	0
2	0	0.0252	−0.491	0.478	−0.768
3	−0.666	0.478	0.478	−1.069	−0.666
L	0	0	−0.768	−0.666	0

(b)

Fig. 16. (a) Triple-mode DR filter with capacitive coupling configuration (b) Its coupling matrix.

In this design example, the basic specification was chosen as 80 MHz ripple bandwidth at 2.5 GHz centre frequency with insertion loss less than 0.17 dB and out-of-band rejection of 25 dB at 2.56 GHz. This requires the design of generalised Chebyshev filter with two finite transmission zeros on the high side. Capacitive input/output coupling probes are used to change the sign of R_{i1} and R_{o2} couplings thus two finite transmission zeros on the high side. Fig. 16 shows a photo of the 3D model of the triple-mode resonator with capacitive coupling configuration and its coupling matrix. The simulation and synthesised frequency response are shown in Fig. 17. The latter configuration can be combined with the triple-mode filter shown in Fig. 9(a) to build contiguous diplexers.

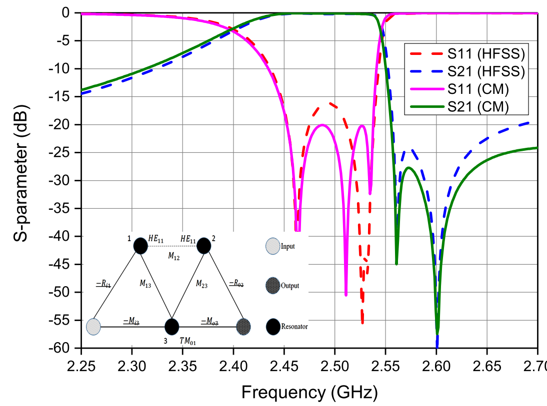

Fig. 17. EM Simulation versus coupling matrix frequency response with two finite transmission zeros on the high side

D. Higher Order Filters

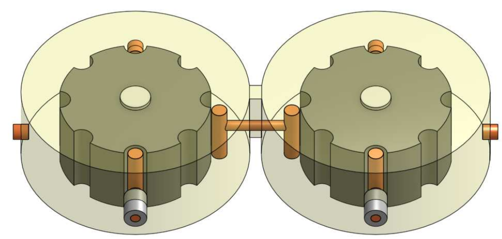

Fig. 18. A six-pole triple-mode dielectric resonator filter.

Higher-order filters are attainable by cascading the basic building block of the triple-mode dielectric resonator. As a design example, a six-pole bandpass filter with centre frequency of 2.5 GHz, ripple bandwidth of 80 MHz, Q-factor of 3600 and four finite transmission zeros on the low side was designed, fabricated and tested. Fig. 18 shows a photo of the 3D model of the six-pole filter. A comparison between the simulation and synthesised frequency response is shown in Fig. 19. A photograph of the fabricated prototype is shown in Fig. 20. A comparison between the simulation and measured frequency response is shown in Fig. 21. It is clear that the measured frequency response is shifted up in frequency by approximately 15 MHz. Again this shift is believed to be due to the fact that the ceramic having a slightly lower dielectric constant than the one assumed in the simulation.

IV. Conclusion

A new class of triple-mode dielectric resonator filters has been described. They offer the advantages of significant size reduction, less than one quarter of the physical volume of equivalent TEM filters, reduced cost and design complexity. The spurious free response of the proposed filter is good, i.e., the first spurious mode happened 650 MHz above the fundamental resonances. The proposed resonator can be implemented as cascaded triplets enabling the design of bandpass

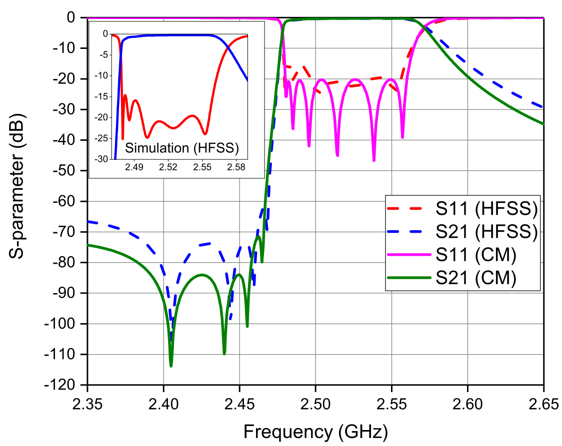

Fig. 19. EM simulation versus coupling matrix frequency response with four finite transmission zeros on the low side.

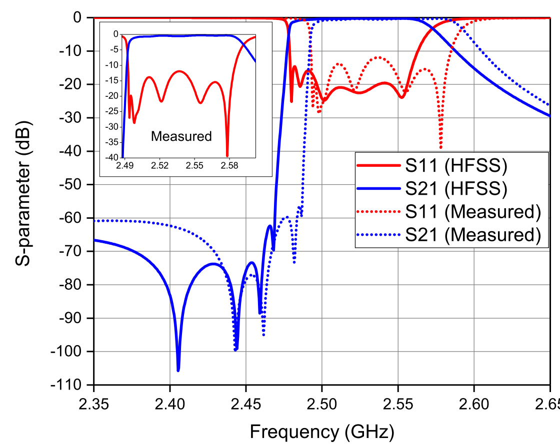

Fig. 21. EM simulation vs measured frequency response with four finite transmission zeros on the lower side.

Fig. 20. Photo of a six-pole bandpass filter with four transmission zeros on the low side.

filters with finite transmission zeros on either or both sides of the passband. Prototype bandpass filters have been designed, fabricated and tested validating the proposed approach. A detailed study of these devices has been carried out to build filters with high-orders, controllable centre frequency, bandwidth and finite transmission zeros.

References

[1] V. Walker and I. C. Hunter, Design of triple mode TE resonator transmission filters, *IEEE Microw. Wireless Compon. Lett.*, vol. 12, no. 6, pp. 215217, Jun. 2002.

[2] I. C. Hunter, J. D. Rhodes, and V. Dassonville, Triple mode dielectric resonator hybrid reflection filters, *Proc. Inst. Elect. Eng.*, vol. 145, no. 4, pp. 337343, Aug. 1998.

[3] L. H. Chua and D. Mirshekar-Syahkal, Analysis of dielectric loaded cubical cavity for triple-mode filter design, *Proc. Inst. Elect. Eng.Microw., Antennas, Propag.*, vol. 151, no. 1, pp. 6166, Feb. 2004.

[4] N. Park et al., Compact triple-mode bandpass filter using spherical dielectric resonator, *2013 European Microwave Conference*, Nuremberg, 2013, pp. 810-813.

[5] U. Rosenberg and D. Wolk, Filter design using in-line triple-mode cavities and novel iris couplings, *IEEE Trans. Microwave Theory Tech.*, vol. 37, pp. 20112019, Dec. 1989.

[6] M. Mohammad-Taheri, D. Mirshekar-Syahkal, and S. SafaviNaieni, Sixth-order elliptic function filter using triple-mode dielectric-loaded cylindrical cavities, *IEE Proc. Microwaves, Antennas Propagat.*, vol. 149, pp. 237-242, 2002.

[7] S. W. Wong, Z. C. Zhang, S. F. Feng, F. C. Chen, L. Zhu and Q. X. Chu, Triple-Mode Dielectric Resonator Diplexer for Base-Station Applications, *in IEEE Transactions on Microwave Theory and Techniques*, vol. 63, no. 12, pp. 3947-3953, Dec. 2015.

[8] M. S. Bakr, F. Gentili and W. Bosch, Triple mode dielectric-loaded cavity band pass filter, *2016 16th Mediterranean Microwave Symposium (MMS)*, Abu Dhabi, 2016, pp. 1-3.

[9] D. R. Hendry and A. M. Abbosh, Analysis of Compact Triple-Mode Ceramic Cavity Filters Using Parallel-Coupled Resonators Approach, *in IEEE Transactions on Microwave Theory and Techniques*, vol. 64, no. 8, pp. 2529-2537, Aug. 2016.

[10] Wai-Cheung Tang and S. K. Chaudhuri, A True Elliptic-Function Filter Using Triple-Mode Degenerate Cavities, *in IEEE Transactions on Microwave Theory and Techniques*, vol. 32, no. 11, pp. 1449-1454, Nov 1984.

[11] S. Amari and U. Rosenberg, New in-line dual- and triple-mode cavity filters with nonresonating nodes, *in IEEE Transactions on Microwave Theory and Techniques*, vol. 53, no. 4, pp. 1272-1279, April 2005.

[12] M. S. Bakr, I. C. Hunter and W. Bosch, Miniature Triple-Mode Dielectric Resonator Filters, *2018 IEEE/MTT-S International Microwave Symposium - IMS*, Philadelphia, PA, USA, 2018, pp. 1249-1252.

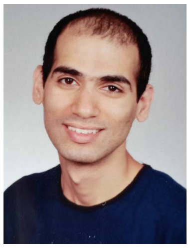

Mustafa S. Bakr (GSM'14) received the B.Sc. degree (Honours, 1st Class) from the University of Technology, Iraq, in 2012, the M.SC. degree (with distinction) from the University of Leeds, UK, in 2015 and the Ph.D. degree (with distinction) from the Graz University of Technology in 2018. His early employment was at the University of Technology, Baghdad, Iraq. Since 2016, he is at the Graz University of Technology, Graz, Austria, and the University of Leeds, UK. He is also with Radio Design Ltd, Shipley, UK. He was the recipient of the IEEE MTT-S Graduate Fellowship Award for the year 2017, Erasmus grant in 2016-17, the best poster award at EWSN2017, and the best demo award at SenSys 2017. He has authored/co-authored several papers, and a book chapter. He has four patents pending. His current research interest includes passive microwave filter and antenna design for IoT and mobile communication. Dr. Bakr is an associate fellow of the Higher Education Academy in the UK, a member of the IEEE, and the IET.

Ian C. Hunter (M82SM94F07) graduated from Leeds University, with BSc Hons 1st Class, 1978 and PhD, 1981. His early employment was at Aercom and KW Engineering, California, and Filtronic, UK, developing broadband microwave filters for EW. applications. From 1995-2001 he was at Filtronic Comtek, working on advanced filters for cellular radio. He held the UK Royal Academy of Engineering/Radio Design Ltd Research Chair in Microwave Signal Processing at the University of Leeds, School of Electronic and Electrical Engineering, Leeds, UK, from 2012 to 2017. He was the author of the IET book Theory and Design of Microwave Filters and is currently leading a team researching new microwave filters for mobile communications systems. He was General Chair of European Microwave Week, Manchester 2011 and chair the of European Microwave Conference, London 2016. Prof Hunter is a Fellow of the IEEE, the IET and the UK Royal Academy of Engineering.

Wolfgang Bsch (F13) received the engineering degree from the University of Technology, Vienna, Austria, the Engineering degree from the Universities of Technology, Graz, Austria, and the M.B.A. degree (with distinction) from the Bradford University School of Management, Bradford, MA, USA, in 2004. He was the CTO with the Advanced Digital Institute, U.K., a not-for-profit organization to promote research activities. Earlier, he served as the Director of Business and Technology Integration with RFMD, U.K. He has been with Filtronic plc, as CTO of Filtronic Integrated Products and the Director of the Global Technology Group for nearly 10 years. Before joining Filtronic, he held positions with the European Space Agency, where he was involved in amplifier linearization techniques; MPRTeltech, Canada, where he was involved in MMIC technology projects; and the Corporate Research and Development Group, M/A-COM, Boston, MA, USA, where he was involved in advanced topologies for high-efficiency power amplifiers. In 2010, he joined the Graz University of Technology, to establish a new Institute for Microwave and Photonic Engineering. For four years, he was with DaimlerChrysler Aerospace (now Airbus), Germany, where he was involved in T/R modules for airborne radar. He was a Nonexecutive Director of Diamond Microwave Devices with the Advanced Digital Institute. He is currently a Nonexecutive Director with the VIPER-RF Company, U.K. He has authored more than 80 papers and holds 4 patents. Prof. Bsch is a Fellow of the IEEE and the IET.